

Study on the Effect of Forming Parameters in Sheet Hydrodynamic Deep Drawing Using FEM-based Taguchi Method

B. Zareh*

Department of Mechanical Engineering,
Babol Noshirvani University of Technology, Iran
E-mail: zareh.behrooz@yahoo.com

*Corresponding author

A. H. Gorji & M. Bakhshi & S. Nourouzi

Department of Mechanical Engineering,
Babol Noshirvani University of Technology, Iran

Received: 9 Mars 2012, Revised: 14 June 2012, Accepted: 29 July 2012

Abstract: In this paper, a FEM-based Taguchi method is used to determine the effects of forming parameters on the quality of part formability in the process of hydrodynamic deep drawing assisted by radial pressure. Four important forming parameters, fluid pressure, friction coefficient at blank/punch interface, die entrance radius and the amount of gap (g) between die rim block and blank holder are considered in this investigation. In order to have more comprehensive study, three different workpieces are used as the case studies. Three-dimensional FE models are developed for simulating the forming process. After experimental validation, these models are used for performing the set of experiments designed by Taguchi's L₉ orthogonal array. The signal-to-noise (S/N) ratio and the analysis of variance (ANOVA) techniques are used to calculate the contributions of each of the mentioned parameters to the output characteristic. The results indicate that fluid pressure and friction coefficient are the most influential parameters. Also, die entrance radius and the amount of gap (g) have considerable effect on the part formability. The obtained results may provide useful guidance on determining forming parameters.

Keywords: Analysis of Variance, Finite Element Simulation, Sheet Hydroforming, Taguchi Method

Reference: Zareh, B., Gorji, A. H., Bakhshi, M. and Nourouzi, S., "Study on the Effect of Forming Parameters in Sheet Hydrodynamic Deep Drawing Using FEM-based Taguchi Method", Int J of Advanced Design and Manufacturing Technology, Vol. 6/ No. 1, pp.87-99.

Biographical notes: **B. Zareh** is PhD student of Mechanical Engineering at University of Tabriz, Iran. His current research interests include Advanced Metal Forming Processes and Dynamic Behavior of Materials. **A. Gorji** is Assistant Professor of Mechanical Engineering at Babol Noshirvani University of Technology, Iran. **M. Bakhshi** is full Professor of Mechanical Engineering at Babol Noshirvani University of Technology, Iran. He received his PhD in Mechanical Engineering from Birmingham University, UK. **S. Nourouzi** is Assistant Professor of Mechanical Engineering at Babol Noshirvani University of Technology, Iran. He received his PhD in Surface Engineering from University of Limoges, France.

1 INTRODUCTION

Sheet hydroforming is a recently developed technology that uses a pressurized fluid medium to deform a workpiece. This process has gained an increasing interest during the last couple of years, especially as application in the manufacturing of some components for automotive, aerospace, and electrical appliances [1], [2]. Sheet hydroforming technology offers several technological advantages in comparison to conventional stamping processes, such as a higher drawing ratio, better surface quality, less springback, fewer secondary operation, better dimensional accuracy and the capability of forming complicated-shaped sheet metal parts [3], [4]. Although this process has many advantages and good application prospects, the usage of liquid in the die cavity makes this process more complicated than conventional deep drawing. Also, in comparison to the conventional deep drawing, further parameters affect the formability of sheet metal during the sheet hydroforming process. For wide application of this technology, there is a need for a fundamental understanding of the influence of forming parameters and their degree of importance on sheet hydroformability, which will be very helpful for spreading this technology in industry and for adding more knowledge into its database.

In recent years, several new sheet hydroforming processes have been introduced such as aquadraw deep drawing, hydromechanical deep drawing, hydrodynamic deep drawing (HDD), hydraulic deep drawing with counter pressure, hydro-form, sheet hydroforming with a movable die, hydrodynamic deep drawing assisted by radial pressure (HDDRP) and hydromechanical deep drawing with uniform pressure on the blank [4-10]. Also, the effect of forming parameters on the sheet hydroforming process has been studied by some researchers using experiments, analytical models and finite element simulations. Hsu and Hsieh [11] developed an analytical model to predict the upper bound and lower bound of the permissible fluid pressure in hemispherical-cup hydroforming process. They found out that the material properties which include the strain hardening and normal anisotropic parameter tend to shift the working zone. Zhang et al. [12] showed that material anisotropy and pre-bulging pressure have a remarkable influence on the final product quality. Lang et al. [13-15] carried out a series of research works on the effects of the key process parameters such as pre-bulging, punch surface roughness and fluid pressure during hydro-mechanical deep drawing with uniform pressure onto the blank. Fazli and Dariani [16] used FEM to study the effect of

process parameters on hydromechanical deep drawing process and gave the conclusion that increasing the friction between blank and die or blank and blank-holder decreases the LDR value. Singh and Kumar [17] investigated the effect of pre-bulging pressure and cut-off pressure on thickness distribution and surface finish in hydro-mechanical deep drawing. However, the pervious researchers have considered the effect of forming parameters independently and consideration of the influence of the forming parameters simultaneously in sheet hydroforming process has not been found in the literature. Also, the previous works have studied the effect of forming parameters only on the hydroformability quality of a workpiece with a specific geometry.

The Taguchi method has been widely applied in various industrial fields including the metal forming area in order to design a robust manufacturing process and determine optimal design parameters [18]–[20]. The Taguchi method adopts a set of standard orthogonal arrays to determine parameters configuration and analysis results. These kinds of arrays use a small number of experimental runs but obtain maximum information and have high reproducibility and reliability. In this paper, finite element method and Taguchi method are combined to analyse the effects of forming parameters on the quality of part formability and determine the optimal combination of forming parameters in sheet hydroforming process. The process of hydrodynamic deep drawing assisted by radial pressure (HDDRP) is employed as an example to apply the proposed approach. In order to have more comprehensive study, three different workpieces are considered as case studies in this investigation. This type of analysis is not available in the literature and will be very helpful to the development and practical application of this technology for a wide range of sheet metal components.

2 METHODOLOGY

Taguchi techniques have been utilized widely in engineering analysis to optimize the performance characteristics within the combination of design parameters. The Taguchi method considers three stages in a process development: (1) system design, (2) parameter design, and (3) tolerance design [21]. The focus of the system design is on determining the suitable working levels of design factors. Parameter design seeks to determine the factor levels that produce the best performance of the product/process under

study. The optimal condition is selected in a way that the influence of uncontrollable factors causes minimum variation of system performance. Tolerance design is a way to fine-tune the results of the parameter design by tightening the tolerance of factors with significant influence on the product. Among these stages, parameter design is the key step in the Taguchi method to achieve high quality without increasing the costs. To obtain high forming performance in the sheet hydroforming process, the parameter design approach proposed by the Taguchi method is adopted in this paper.

The purpose of this study is to investigate the influence of forming parameters on the hydroformability to improve the hydroformed sheet quality. In order to achieve above target, first, the objective function is defined and the forming parameters are selected, and the appropriate orthogonal array is constructed. Then, the three-dimensional finite element (FE) model is developed for simulating the HDDRP process using dynamic explicit, commercial code, Abaqus 6.7.1. In order to validate the FE models, thickness distribution curves and punch load-stroke curves of the experimentally formed cups are compared with the predicted values. These validated models are then used to carry out virtual experiments for each set of forming parameters designed by Taguchi's standard orthogonal array. Then, the virtual experimental results are transformed into the Taguchi's signal-to-noise (S/N) ratios and the optimal parameters are obtained. Finally, Statistical analysis of variance (ANOVA) is performed to see which parameters are significant.

3 HYDRODYNAMIC DEEP DRAWING ASSISTED BY RADIAL PRESSURE (PROCESS DESCRIPTION)

The process of hydrodynamic deep drawing assisted by radial pressure (HDDRP) is shown in Fig. 1, which is developed from the conventional hydrodynamic deep drawing (HDD) through a little modification of the tool setup. In the HDDRP process, when the punch goes down into the die cavity, the pressurized liquid in the die cavity will push the blank tightly onto the punch surface. In the meantime, the liquid in the die cavity may flee out from the gap between the blank and the die. At the same time, because the gap g where the liquid flees out is very small, a liquid pressure exists around the blank rim. This is different from conventional HDD process [22]. The HDDRP process has many forming parameters involved in affecting its hydroformability. So, in the present research, this process is taken as an example to implement previously mentioned procedure.

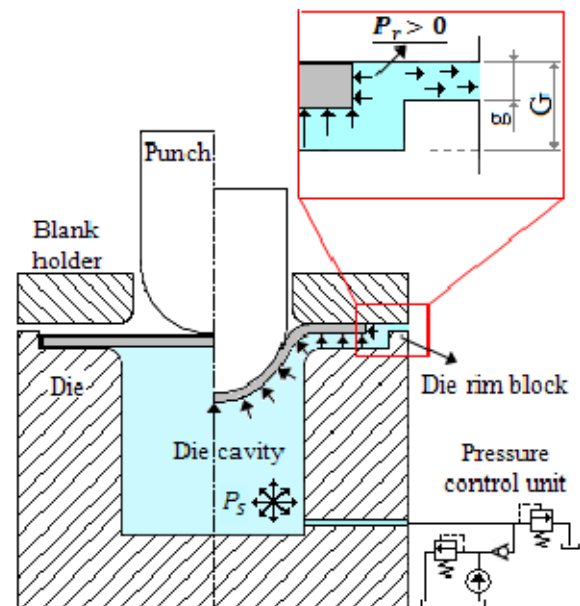


Fig. 1 Schematic representation of hydrodynamic deep drawing assisted by radial pressure.

4 SELECTION OF THE FORMING PARAMETERS AND CONSTRUCTION OF THE ORTHOGONAL ARRAY

Sheet hydroforming process and the quality of the formed parts can be influenced by many forming parameters. Generally, there are three categories of parameters influencing hydroformability, i.e., geometry parameters, material parameters, and process parameters. Based on the previous study reported by Sharma and Rout [23], for the entire range of a specific material, the influence of material properties such as strain hardening exponent and plastic anisotropy ratio is less than other forming parameters. Moreover, in most cases for a specific workpiece, there is a little flexibility in material selection. Hence, the process parameters and geometry parameters are taken into account in this study. Among all process parameters and geometry parameters, fluid pressure in the die cavity (P_s), interfacial friction condition between blank and punch surface and die entrance radius are the most important parameters that can affect the sheet hydroformability during the sheet hydroforming process. Also, in HDDRP process the amount of gap (g) has a great influence on the process window. Therefore, these parameters are taken into account in this investigation. To evaluate, three levels are selected for each of the above mentioned parameters. Table 1

shows the selected parameters and their levels used in FE simulation. For four factors with three levels for each, the experimental layout of L₉ orthogonal array, which has 9 rows corresponding to the number of tests (8 degree of freedom), is selected for present research according to Taguchi's suggestion [24]. Table 2 shows the L₉ orthogonal array in which 9 runs are carried out to investigate the effects of the four selected factors.

Table 1 Parameters and their levels

Parameters	Level 1	Level 2	Level 3
A: Fluid pressure (MPa)	10	20	30
B: Friction coefficient (μ)	0.08	0.14	0.20
C: Gap (g) (mm)	0.00	0.05	0.10
D: Die entrance radius (mm)	3.00	4.00	5.00

Table 2 Taguchi's L₉ orthogonal array

Ex. no.	A	B	C	D
1	1	1	1	1
2	1	2	2	2
3	1	3	3	3
4	2	1	2	3
5	2	2	3	1
6	2	3	1	2
7	3	1	3	2
8	3	2	1	3
9	3	3	2	1

Considering the widespread applications of cylindrical, hemispherical and parabolic work pieces in the fields of aviation, aerospace, automobile industry, etc., in this work, hydroforming of these parts are considered as the case studies to investigate the effects of mentioned parameters. Hence, the set of simulations designed by Taguchi's L₉ orthogonal array are carried out for each of the three considered case studies. Therefore, 27 finite element simulation runs are performed in this study.

Although there are many different proposed criteria for predicting fracture in sheet metal formed parts, there is no standard approach. Therefore, the commonly used thinning ratio criteria is used here as a measure of forming quality. The thinning ratio is defined by:

$$\text{Thinning ratio (\%)} = \frac{t_0 - t_1}{t_0} \times 100 \quad (1)$$

where t_0 is the original thickness of the sheet and t_1 is the critical thickness of the hydroformed cup.

5 FINITE ELEMENT SIMULATION MODEL

In this study, finite element simulation is used as a substitute tool for experimental tests. The commercial finite element software, ABAQUS/Explicit 6.7 is used for simulation of the HDDRP process. The FE models are shown in Fig. 2 in an exploded view. As shown in the Fig. 2, only a quarter of the blank and the tool components are modeled due to symmetry. The dimension of the initial blank and the tool components are listed in Table 3. According to Fig. 1, in HDDRP process a radial pressure is loaded onto the blank rim to push the blank forward. But in general finite element softwares, the pressure vector vertical to the normal of one shell element cannot be supplied to the element. So, in order to apply the radial pressure onto the blank rim, the blank is modeled as a solid deformable body and is meshed with eight-node solid elements C3D8R. The applied material is St14 steel sheet with 1 mm thickness. The necessary blank material properties which are obtained from tensile test are given in Table 4. The tool components are modeled as rigid surfaces using discrete rigid surface elements R3D4. The Coulomb's friction law model is applied to define the friction contact condition between the interfaces. The friction coefficient at blank/blank holder and blank/die interfaces is considered to be 0.05. According to the input parameters sets designed by Taguchi's L₉ orthogonal array, the friction coefficient at blank/punch interface is taken as $\mu=0.08, 0.14$ or 0.20 .

Table 3 Dimension of the tool components

Parameter	Value (mm)
Punch diameter	41.8
Die inside diameter	44
Die entrance radius	3
Blank holder inside diameter	41.9
Blank holder entrance radius	3
Initial blank diameter (mm)	80

Table 4 Mechanical properties of the St14 steel sheet

Parameter	Value
Young modulus, E (GPa)	210
Yield stress, σ (MPa)	175
Strain-hardening exponent, n	0.36
Strength coefficient, K (MPa)	648.53
Poisson's ratio ν	0.30
Normal anisotropy \bar{R}	1.53

The amount of gap (g) is one of the parameters that is investigated in this study. This parameter directly affects the amount of radial pressure loaded onto the

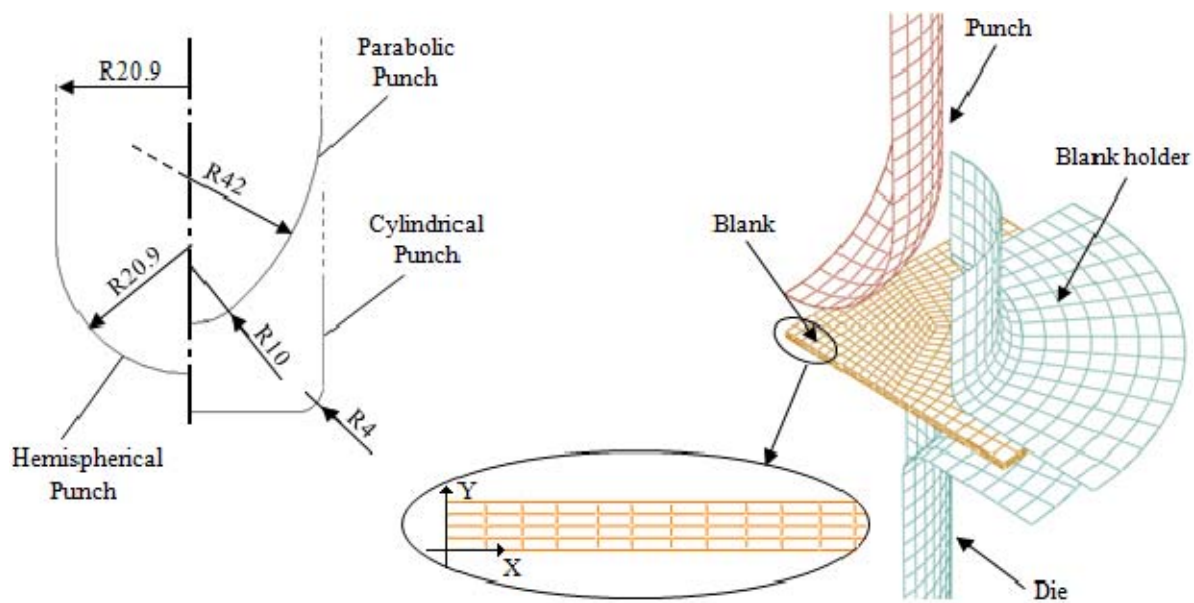


Fig. 2 The exploded view of the FEM models (one-quarter geometry).

blank rim. Based on reference [22] for the specified range of gap (g) following Eq. (2) is used to calculate this pressure in the simulations:

$$P_r = \frac{6\eta Q}{\pi g^3} \ln\left(\frac{R}{a}\right) \quad (2)$$

Where P_r is the liquid pressure along the rim of the blank, η the dynamic viscosity of the liquid, Q the flow rate, g the gap, R the external radius for the gap and a is the internal radius for the gap. These parameters are shown in Fig. 3. The appropriate levels for the gap g are selected in a way that the amount of radial pressure varies from $P_r \approx P_s$ to $P_r \approx 0$.

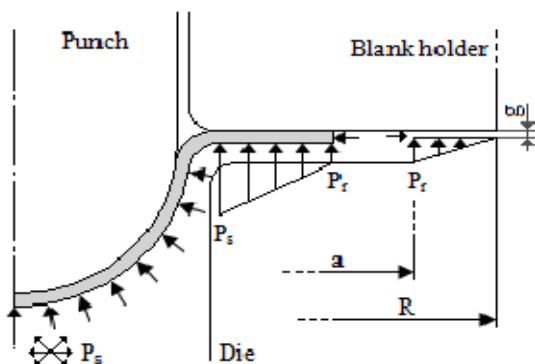


Fig. 3 The fluid pressure distribution on the flange area during the forming process [22]

In HDDRP process, liquid pressure in the die cavity varies during the forming process. Also, the liquid pressure distribution under flange region is non-uniform, shown in Fig. 3. So, in the FE model the pressure distribution under the blank must be defined as a function of nodes coordinates and time. ABAQUS/Explicit can be applied in combination with the VDLOAD subroutine. This subroutine can be used to define the variation of the distributed load magnitude as a function of position, time, velocity, etc [25]. Thus, VDLOAD subroutine is used for modeling the fluid pressure.

6 EXPERIMENTAL PROCEDURE AND VALIDATION OF THE FE MODEL

A Denison Mayes Group universal testing machine with 600-kN capacity is used in the experiments. Fig. 4 shows the experimental equipment and the manufactured die set mounted on the test machine. The pressure generating system is a hydraulic unit with a maximum capacity of 35 MPa. The working pressure is regulated by a pressure relief valve. Fig. 5 shows the formed parts. In order to verify the validity of developed FE model, the thickness distribution and punch force variations of the formed parts in the experimental tests are compared with those obtained from the finite element simulations. These comparisons are shown in Fig. 6 and 7, respectively. As can be

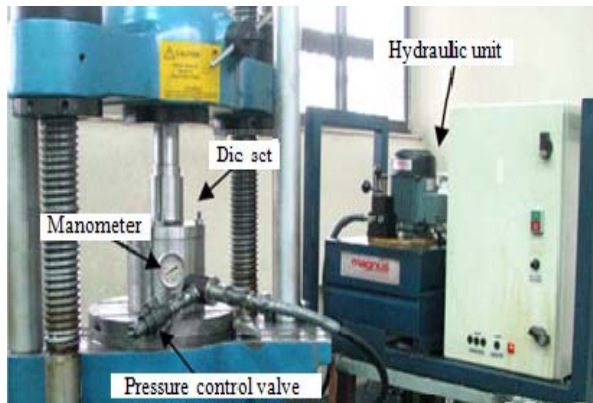


Fig. 4 Experimental equipment and the manufactured die set

inferred from the figures, the finite element results are in good agreement with the experimental results and hence the developed FE model can be used as a proper substitute tool for performing the set of experiments designed by Taguchi's L₉ orthogonal array.



Fig. 5 Photograph of the hydroformed work pieces obtained from experiments (a) parabolic cup, (b) hemispherical cup, (c) cylindrical cup

7 RESULTS AND DISCUSSION

Three different sheet metal parts, cylindrical cup, hemispherical cup and parabolic cup were considered as the case studies in this investigation. Finite element simulations were performed for each of the above mentioned parts according to the arrangements of Taguchi's L₉ orthogonal array (Table 2). The results obtained from finite element simulations were then transformed into signal-to-noise (S/N) ratio. The significance of the design factors were estimated by the analysis of variance (ANOVA) statistical method.

7.1. S/N Analysis

Taguchi's method uses a statistical measure of performance called signal-to-noise ratio (S/N), which is logarithmic function of desired output to serve as objective functions for optimization [24]. It is defined as the ratio of the mean (signal) to the standard deviation (noise). The ratio depends on the quality characteristics of the product/process to be optimized. There are three categories of performance characteristics in the analysis of the S/N ratio: the lower-the-better (LB), the higher-the-better (HB), and the nominal-the-better (NB). The S/N ratio is expressed as:

$$S / N = -10 \log(MSD) \quad (3)$$

where MSD is the mean squared deviation from the target value of the quality characteristic. For the case of minimization of maximum thinning ratio, LB characteristic needs to be used. The MSD for the lower-the-better quality characteristic can be expressed as:

$$MSD = \frac{1}{n} \sum_{i=1}^n y_i^2 \quad (4)$$

where y_i is the measured value of the lower-the-better quality characteristic and n is the total number of tests for a trial condition.

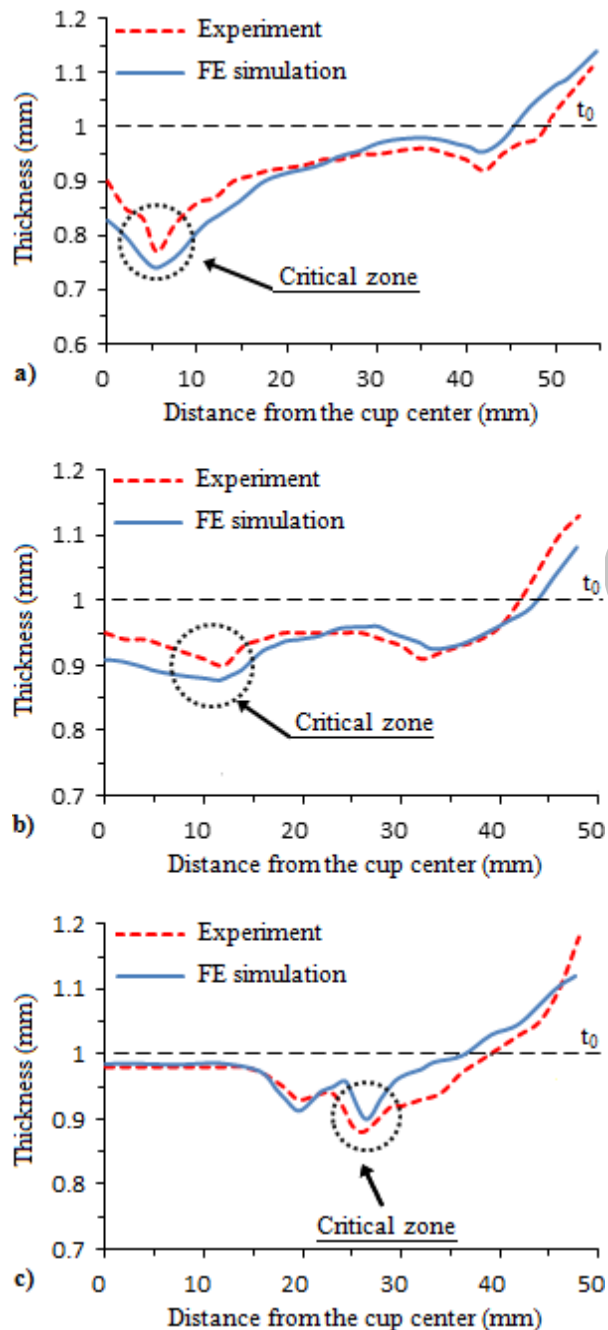


Fig. 6 Comparison of the thickness distribution curves obtained by the experiment and FE simulation (a) parabolic cup, (b) hemispherical cup, (c) cylindrical

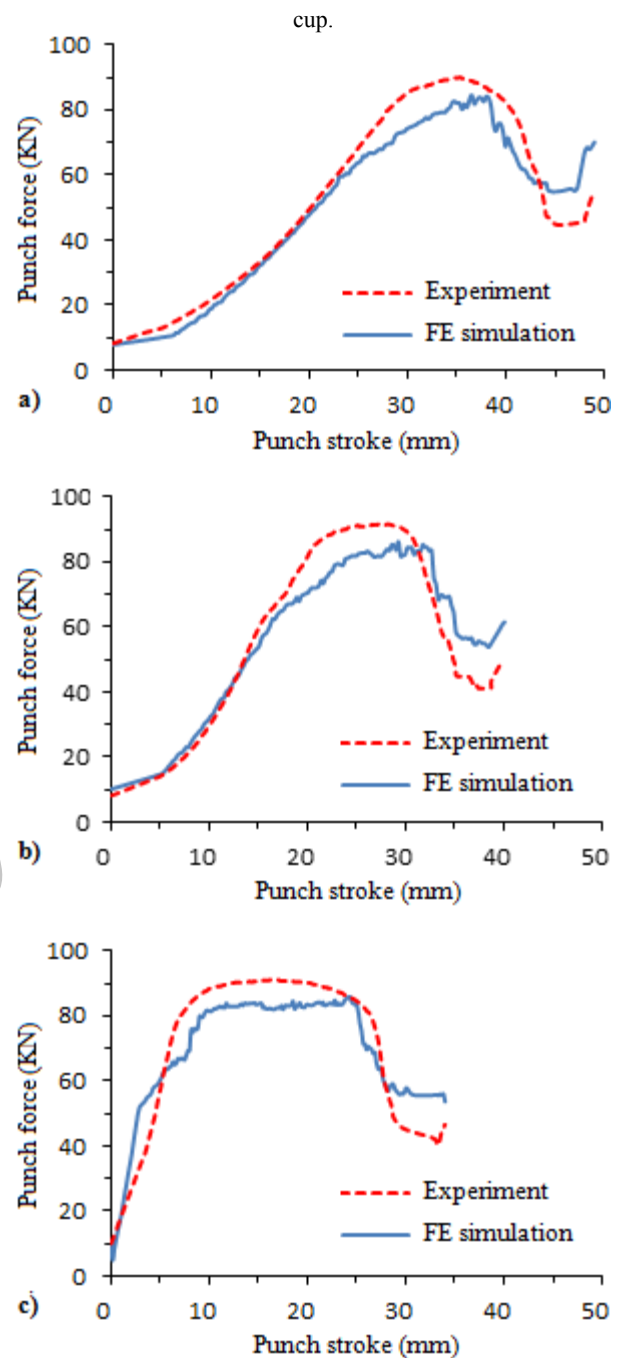


Fig. 7 Comparison of the punch load-stroke curves obtained by the experiment and FE simulation (a) parabolic cup, (b) hemispherical cup, (c) cylindrical cup

Table 5 shows the finite element simulation results for the maximum thinning ratio and its corresponding S/N ratio for the three different hydroformed parts in 9 trial conditions. Since the experimental design is orthogonal, the effect of each control factor on the S/N ratio at different levels can be separated out. The average S/N ratio of each parameter at levels 1 to 3, for

parabolic cup, hemi-spherical cup and cylindrical cup are listed in Tables 6, 7 and 8, respectively. The corresponding main effect plots are also shown in Fig. 8. Regardless of the category of the quality characteristic, a greater S/N ratio corresponds to better quality characteristics. Therefore, the optimal level of

the process parameters is the level with the greatest S/N ratio. According to the Fig. 8, the optimal process parameters combination for minimization of the maximum thickness reduction of parabolic cup, hemispherical cup and cylindrical cup are obtained as A2B3C1D3, A2B3C1D3 and A1B3C1D3, respectively.

Table 5 Experimental results for maximum thinning and S/N ratios

Run.N	Parabolic cup		Hemispherical cup		Cylindrical cup	
	Thinning ratio	S/N ratio	Thinning ratio	S/N ratio	Thinning ratio	S/N ratio
1	0.28297	10.9651	0.13901	17.1390	0.12633	17.9696
2	0.27194	11.3102	0.13020	17.7077	0.11633	18.6857
3	0.25900	11.7338	0.12513	18.0527	0.11053	19.1303
4	0.26240	11.6205	0.11781	18.5763	0.11811	18.5536
5	0.24844	12.0953	0.10794	19.3363	0.12728	17.9044
6	0.21898	13.1917	0.08486	21.4259	0.11053	19.1298
7	0.27094	11.3425	0.13001	17.7204	0.13769	17.2218
8	0.23736	12.4917	0.08993	20.9212	0.11886	18.4987
9	0.23750	12.4867	0.09939	20.0531	0.13411	17.4503

Table 6 S/N response table for maximum thinning ratio (Parabolic cup)

Parameter		Level 1	Level 2	Level 3	[Max-Min]
A	Mean Th. ratio	0.27130	0.24327	0.24860	0.02803
	Mean S/N ratio	11.3364	12.3025	12.1070	0.96615
B	Mean Th. ratio	0.27210	0.25258	0.23849	0.03361
	Mean S/N ratio	11.3094	11.9658	12.4707	1.16138
C	Mean Th. ratio	0.24643	0.25728	0.25946	0.01302
	Mean S/N ratio	12.2162	11.8058	11.7239	0.49231
D	Mean Th. ratio	0.25630	0.25395	0.25292	0.00338
	Mean S/N ratio	11.8490	11.9481	11.9487	0.09965

Table 7 S/N response table for maximum thinning ratio (Hemispherical cup)

Parameter		Level 1	Level 2	Level 3	[Max-Min]
A	Mean Th. ratio	0.13144	0.10353	0.10644	0.02791
	Mean S/N ratio	17.6332	19.7795	19.5649	2.14633
B	Mean Th. ratio	0.12894	0.10935	0.10312	0.02581
	Mean S/N ratio	17.8119	19.3217	19.8439	2.03198
C	Mean Th. ratio	0.10460	0.11580	0.12102	0.01642
	Mean S/N ratio	19.8287	18.7790	18.3698	1.45888
D	Mean Th. ratio	0.11544	0.11503	0.11095	0.00448
	Mean S/N ratio	18.8428	18.9513	19.1834	0.34059

Table 8 S/N response table for maximum thinning ratio (Cylindrical cup)

Parameter		Level 1	Level 2	Level 3	[Max-Min]
A	Mean Th. ratio	0.11773	0.11864	0.13022	0.01249
	Mean S/N ratio	18.5952	18.5293	17.7236	0.87157
B	Mean Th. ratio	0.12738	0.12082	0.11839	0.00898
	Mean S/N ratio	17.9150	18.3629	18.5701	0.65512
C	Mean Th. ratio	0.11857	0.12285	0.12516	0.00659
	Mean S/N ratio	18.5327	18.2299	18.0855	0.44722
D	Mean Th. ratio	0.12924	0.12152	0.11583	0.01340
	Mean S/N ratio	17.7748	18.3457	18.7275	0.95275

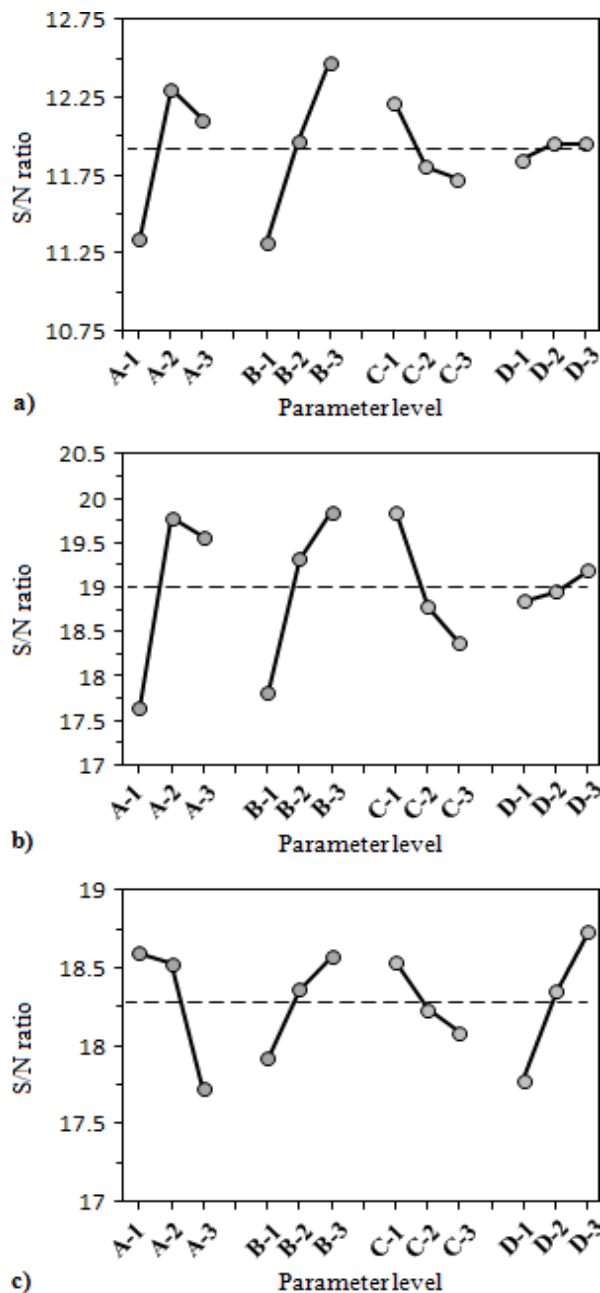


Fig. 8 Main effect plots (a) parabolic cup, (b) hemispherical cup, (c) cylindrical cup

7.2. Analysis of variance (ANOVA)

The Taguchi experimental analysis provides the information not only for the selection of an optimal condition, but also for the evaluation of the relative importance of each factor for further studies. The analysis of variance (ANOVA) procedure is used to quantify the influence of the forming parameters on the quality characteristic. ANOVA separates the overall variation from the average S/N ratio into contribution by each of the parameters and the error. First, the total

sum of the squared deviations SS_T from the total mean S/N ratio can be calculated as [26]:

$$SS_T = \sum_{i=1}^m \left(\frac{S}{N} \right)_i^2 - \frac{1}{m} \left[\sum_{i=1}^m \left(\frac{S}{N} \right)_i \right]^2 \quad (5)$$

where m is the number of experiments in the orthogonal array and $(S/N)_i$ is the S/N ratio of the i_{th} experiment. The sum of the squares due to the variation from the total mean S/N ratio for the p_{th} parameter is expressed as:

$$SS_P = \sum_{j=1}^l \frac{\left(\left(\frac{S}{N} \right)_j \right)^2}{t} - \frac{1}{m} \left[\sum_{i=1}^m \left(\frac{S}{N} \right)_i \right]^2 \quad (6)$$

where l is the number of the parameter levels ($l = 3$ in this study), j is the level number of this specific parameter p , $(S/N)_j$ is the sum of the S/N ratio involving this parameter p and level j , and t is the repetition of each level of parameter p . The percentage contribution of the p_{th} parameter can be calculated as:

$$P_P (\%) = \frac{SS_P}{SS_T} \times 100 \quad (7)$$

The results of ANOVA for the parabolic cup, hemispherical cup and cylindrical cup are shown in Tables 9 to 11, respectively. Based on the ANOVA results given in Table 9, the friction coefficient at blank/punch interface (50.39%) is the most significant parameter influencing the maximum thinning ratio of the parabolic cup followed by fluid pressure and the amount of gap g . Die entrance radius has the least effect on the maximum thinning ratio and is assumed to be negligible and is pooled to form the error variance estimate. In the case of hemispherical cup the fluid pressure (44.96 %) is found to be the most significant parameter influencing the maximum thinning ratio, as shown in Table 10. Following this, the descending order of contributions are the friction coefficient at blank/punch interface and the amount of gap g . Die entrance radius again has the least contribution and is pooled. Table 11 shows the results of ANOVA for the cylindrical cup. It is seen that the fluid pressure (37.40 %) and die entrance radius (36.51 %) have got the most significant influence on the maximum thinning ratio of the cylindrical cup while the friction coefficient and the amount of gap g have also got strong influence on the maximum thinning ratio of the cylindrical cup.

Table 9 Analysis of variance table for maximum thinning ratio (Parabolic cup)

Factor	Degree of freedom	Sum of square	Mean square	Contribution (%)
A	2	1.5655	0.7827	38.7545
B	2	2.0346	1.0173	50.3955
C	2	0.4175	0.2087	10.3406
*D	2	0.0197	0.0098	0.4892
Error	0			
Total	8	4.0374	2.0187	100
(Error)	2	0.0790	0.0395	1.9570

*Factors used for pooling

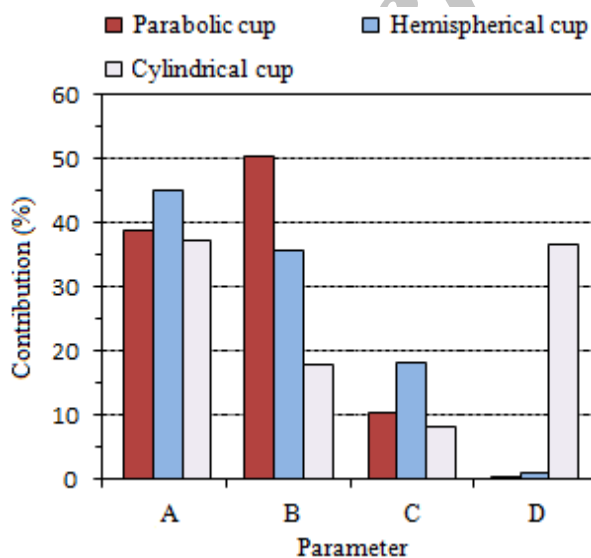
Table 10 Analysis of variance table for maximum thinning ratio (Hemispherical cup)

Factor	Degree of freedom	Sum of square	Mean square	Contribution (%)
A	2	8.3844	4.1922	44.9691
B	2	6.6811	3.3405	35.8339
C	2	3.3976	1.6988	18.2227
*D	2	0.1816	0.0908	0.9741
Error	0			
Total	8	18.6448	9.3224	100
(Error)	2	0.72654	0.36327	3.8967

*Factors used for pooling

Table 11 Analysis of variance table for maximum thinning ratio (Cylindrical cup)

Factor	Degree of freedom	Sum of square	Mean square	Contribution (%)
A	2	1.4130	0.7065	37.4035
B	2	0.6727	0.3363	18.8078
C	2	0.3125	0.1562	8.2736
D	2	1.3795	0.6897	36.5149
Error	0			
Total	8	3.7779	1.8889	100

**Fig. 9** Comparison of the relative contribution of each factor among the three different case studies

The percentage contribution of the selected factors and their optimal levels are compared among the three different formed cups, which are shown in Fig. 9 and Table 12, respectively. The optimal level of various factors and their relative contributions on the maximum thinning ratio in both parabolic cup and hemispherical cup are almost the same while the results for cylindrical cup are a little different. From Fig. 9, it can be inferred that the fluid pressure is one of the first two significant factors for all the three formed cups. As shown in Fig. 8, for the parabolic cup and hemispherical cup by increasing the fluid pressure, the maximum thinning ratio initially decreases, but then after a certain level the maximum thinning ratio increases slowly again. The high contribution of this factor is due to the fact that increasing the fluid pressure to a certain value increases the useful friction holding effect between the punch and the blank during the forming process, which can decrease the maximum thinning ratio of the formed cups considerably.

Table 12 Comparison of the optimal level of each factor among the three different case studies

Parameter	Optimum level		
	Parabolic cup	Hemispherical cup	Cylindrical cup
A: Fluid pressure	2	2	1
B: Friction coefficient	3	3	3
C: Gap (g)	1	1	1
D: Die entrance radius	3	3	3

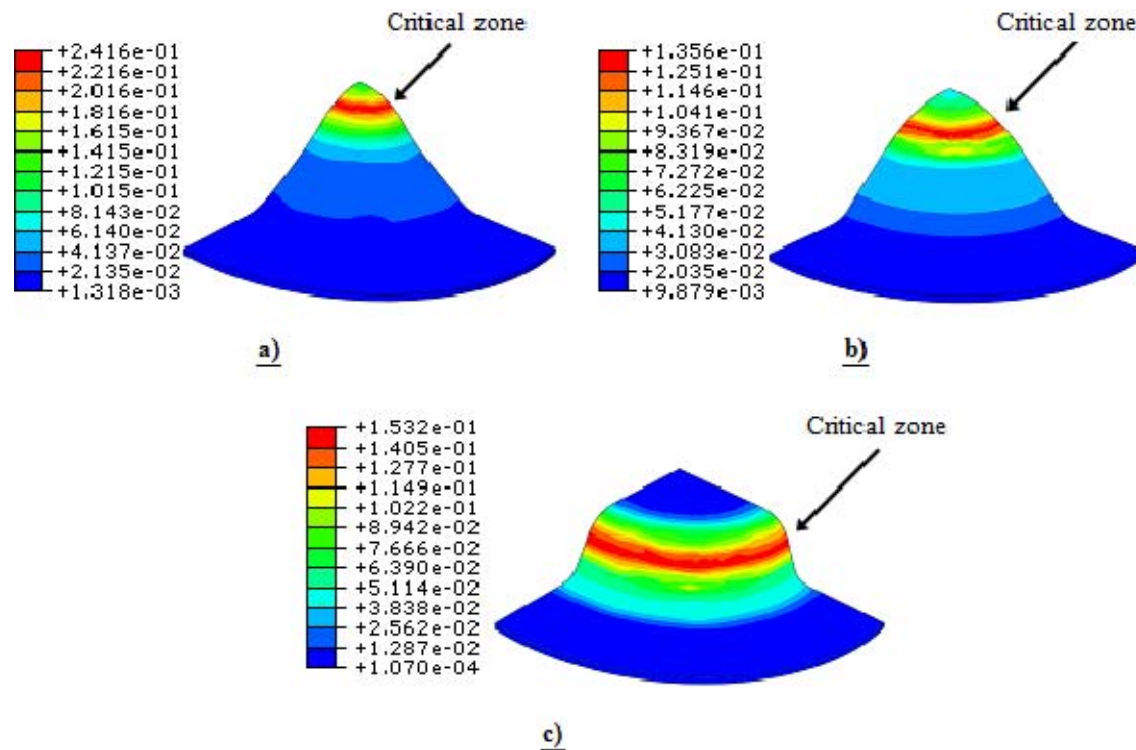


Fig. 10 Maximum principle plastic strain distribution of the formed parts (a) parabolic cup, (b) hemispherical cup, (c) cylindrical cup

By considering the results of Table 12 and Fig. 8, it can be concluded that the amount of maximum thinning ratio decreases with the increase of the friction coefficient at blank/punch interface. This trend is in agreement with the observations reported in reference [27]. Another phenomenon that can be inferred from Fig. 9 is that the relative contribution of this factor shows a clear decreasing trend with the change of the geometry of the formed cups from parabolic cup to cylindrical cup. As it is shown in Fig. 10, in the parabolic cup and hemispherical cup, strain is concentrated near the punch nose while the critical zone of the cylindrical cup is at the cup wall near the punch profile. Thus, for dome shaped parts, specially for the parabolic cup the maximum thinning takes place at the punch nose during the first one third of the drawing stage. Higher friction coefficient at blank/punch interface can reduce the tension at the

punch nose, spread the strain over a greater area, move the critical zone from the punch nose to the cup's body and finally reduce the maximum thinning ratio in the formed cup. Therefore, a small increase in the amount of friction coefficient at blank/punch interface can reduce the maximum thickness reduction in dome shaped parts significantly. As it can be seen from Tables 6 to 8, the maximum difference between the average S/N ratios of the friction coefficient at blank/punch interface, is $|0.23849-0.27210| = 0.03361$ for the parabolic cup which is higher than those obtained for hemispherical cup ($|0.10312-0.12894| = 0.02581$) and cylindrical cup ($|0.11839-0.12738| = 0.00898$). This result indicates that compared to hemispherical and cylindrical cups, maximum thinning in the parabolic cup is more sensitive to the effect of friction coefficient at blank/punch interface, and a greater improvement in maximum thinning can be

obtained for this cup by increasing the friction coefficient at blank/punch interface. Therefore, it can be concluded that as the geometry of punch head gets sharper, the degree of importance of the friction coefficient at blank/punch interface increases consequently. The parameter of gap (g) has a similar effect on the maximum thickness reduction of all the three formed cups. As it is shown in Table 12 and Fig. 8, it is obvious that the maximum thinning ratio of the formed cups can be decreased by decreasing the amount of gap (g). Based on Eq. (2), by decreasing the amount of gap (g), higher radial pressure is loaded onto the rim of the blank which can decrease the drawing force and facilitate material flow into the die cavity. Therefore, less thickness reduction will occur in the formed cups and accordingly the drawing ratio will increase. Die entrance radius is found to have less contribution on the maximum thickness reduction in the parabolic and hemispherical cups compared to that in the cylindrical cup. As it is shown in Fig. 9, this factor has a negligible effect on the parabolic and hemispherical cups, because, as illustrated in Fig. 10(a) and (b), in these cups the critical zone is at the punch head and hence the thickness reduction in the critical zone is free from any bending and unbending effect. But as shown in Fig. 10(c), the critical zone of the cylindrical cup is at the cup wall near the punch profile radius where bending and unbending takes place during the forming process. This leads to larger deformation and causes more thickness reduction in this zone. Therefore, die entrance radius has a significant influence on the maximum thinning ratio of the cylindrical cup. As it can be seen from Table 12 and Fig. 8, maximum thickness reduction of the formed cups decreases with the increase of the die entrance radius.

8 CONCLUSION

In this paper, by integrating FE method and Taguchi technique, a systematic method has been provided to evaluate the effects of forming parameters on the quality of part formability in the process of hydrodynamic deep drawing assisted by radial pressure. Also, the analysis of variance (ANOVA) was used to quantify the influence of the forming parameters on the quality characteristic. In order to have more comprehensive study, three different case studies were considered in this investigation. Hence, the results obtained from this study can be used for a wide range of industrial parts. The main conclusions

obtained through this research are summarized as follows:

- 1- For all the three case studies fluid pressure in the die cavity is one of the first two significant factors. Thus, the appropriate choice of this factor is very crucial for minimizing thickness thinning of the formed parts and accordingly achieving a higher drawing ratio.
- 2- The results of ANOVA revealed that friction coefficient at blank/punch interface is also a very important factor. The maximum thinning ratio decreases by increasing the friction coefficient at blank/punch interface. The comparison of the results of S/N and ANOVA analysis among the three formed cups indicated that as the geometry of punch head gets sharper, the degree of importance of this factor increases consequently.
- 3- The maximum thinning ratio of the formed cups decreases by decreasing the amount of gap (g), which means that increasing the radial pressure always has a positive influence on the hydroformability of the sheet during the HDDRP process.
4. It is shown that die entrance radius has a negligible effect on the parabolic and hemispherical cups, while for the cylindrical cup, it is found to be the second most influential factor affecting the maximum thinning ratio. This phenomenon can be attributed to the difference in their critical zones.
- 5- Based on the results from ANOVA analysis, further optimization of the forming parameters can be done based on the degree of importance of the factors on the sheet hydroformability.

REFERENCES

- [1] Zhang, SH., and Danckert, J., "Development of hydro-mechanical deep drawing", *Journal of Material Processing Technology*, Vol. 83, 1998, pp. 14-25.
- [2] Lang, LH., Wang, ZR., Kang, DC., Yuan, S.J., Zhang, S.H., Dankert, J., and Nielsen, K.B., "Hydroforming highlights: sheet hydroforming and tube hydroforming", *Journal of Material Processing Technology*, Vol. 151, 2004, pp. 165-177.
- [3] Kandil, A., "An experimental study of hydroforming deep drawing", *Journal of Material Processing Technology*, Vol. 134, 2003, pp. 70-80.
- [4] Zhang, SH., Wang, ZR., Xu, Y., Wang, Z. T., and Zhou, L. X., "Recent developments in sheet hydroforming technology", *Journal of Material Processing Technology*, Vol. 151, 2004, pp. 237-241.
- [5] Thiruvarduchelvan, S., and Travis, FW., "Hydraulic-pressure enhanced cup-drawing processes-an appraisal", *Journal of Material Processing Technology*, Vol. 140, 2003, pp. 70-75.
- [6] Zhang, SH., Zhou, LX., Wang, ZT., and Xu, Y., "Technology of sheet hydroforming with a movable

- female die”, International Journal of Machine Tools & Manufacture, Vol. 43, 2003, pp. 781-785.
- [7] Lang, L., Danckert, J., and Nielsen, KB., “Investigation into hydrodynamic deep drawing assisted by radial pressure Part I. Experimental observations of the forming process of aluminum alloy”, Journal of Material Processing Technology, Vol. 148, 2004, pp. 119-131.
- [8] Lang, L., Danckert, J., and Nielsen, KB., “Study on hydromechanical deep drawing with uniform pressure onto the blank”, International Journal of Machine Tools & Manufacture, Vol. 44, 2004, pp. 495-502.
- [9] Gorji, A. H., Alavi, H., Bakhshi, M., Nourouzi, S., and Hosseinipour, S. J., “Investigation of hydrodynamic deep drawing for conical-cylindrical cups”, International Journal of Advance Manufacturing Technology, Vol. 56, 2011, pp. 915-927.
- [10] Gorji, A. H., Alavi, H., Bakhshi, M., Valizadeh, M. E., and Shirkorshidian, A., “Finite Element Simulation and Experimental Study of Forming Conical Parts Using Hydrodynamic Deep Drawing with Radial Pressure”, Journal of Mechanic and Aerospace- Emam Hossien Uni (in Persian), Vol. 5(3), 2009, pp. 69-79.
- [11] Hsu, T. C., and Hsieh, S. J., “Theoretical and experimental analysis of failure for the hemisphere punch hydroforming processes”, Journal of Manufacturing Science and Engineering, Vol. 118, 1996, pp. 434-438.
- [12] Zhang, SH., Jensen, MR., Nielsen, KB., Danckert, J., Lang, L., and Kang, D. C., “Effect of anisotropy and prebulging on hydromechanical deep drawing of mild steel”, Journal of Material Processing Technology, Vol. 142, 2003, pp. 544-550.
- [13] Lang, L., Danckert, J., and Nielsen, KB., “Investigation into the effect of pre-bulging during hydromechanical deep drawing with uniform pressure onto the blank”, International Journal of Machine Tools & Manufacture, Vol. 44, 2004, pp. 649-657.
- [14] Lang, L., Danckert, J., and Nielsen, KB., “Analysis of key parameters in sheet hydroforming combined with stretching forming and deep drawing”, Proc IMechE B Journal of Engineering Manufacture, Vol. 218, 2004, pp. 845-856.
- [15] Lang, L., Li, T., Zhou, X., Danckert, J., and Nielsen, KB., “The effect of the key process parameters in the innovative hydroforming on the formed parts”, Journal of Material Processing Technology, Vol. 187-188, 2007, pp. 304-308.
- [16] Fazeli, A., and Dariani, BM., “Parameter study of the axisymmetric hydromechanical deep drawing process”, Proc IMech E B Journal of Engineering Manufacture, Vol. 220, 2006, pp.1937-1944.
- [17] Singh, SK., and Kumar, DR., “Effect of process parameters on product surface finish and thickness variation in hydro-mechanical deep drawing”, Journal of Material Processing Technology, Vol. 204, 2008, pp. 169-178.
- [18] Lee, S.W., “Study on the forming parameters of the metal bellows”, Journal of Material Processing Technology, Vol. 130-131, 2002, pp. 47-53.
- [19] Davidson, MJ., Balasubramanian, K., and Tagore, GRN., “Experimental investigation on flow-forming of AA6061alloy—A Taguchi approach”, Journal of Material Processing Technology, Vol. 200, 2008, pp. 283-287.
- [20] He, X., Yu, Z., and Lai, X., “Robust parameters control methodology of microstructure for heavy forgings based on Taguchi method”, Journal of Materials and Design, Vol. 30, 2009, pp. 2084-2089.
- [21] Roy, R., A Primer on the Taguchi Method, 1nd ed., New York, Van Nostrand Reinhold, 1990.
- [22] Lang, L., Danckert, J., and Nielsen, KB., “Investigation into hydrodynamic deep drawing assisted by radial pressure Part II. Numerical analysis of the drawing mechanism and the process parameters”, Journal of Material Processing Technology, Vol. 166, 2005, pp. 150-161.
- [23] Sharma, A. K., and Rout, D. K., “Finite element analysis of sheet Hydromechanical forming of circular cup”, Journal of Material Processing Technology, Vol. 209, 2009, pp. 1445-1453.
- [24] Roy, RK., Design of Experiment Using Taguchi Approach: 16 Steps to Product and Process Improvement, 1nd ed., Wiley Inter science, New York, 2001.
- [25] ABAQUS Inc, ABAQUS/Explicit User’s Manual. Version 6.7, 2007.
- [26] Nalbant, M., Gokkaya, H., and Sur, G., “Application of Taguchi method in the optimization of cutting parameters for surface roughness in turning”, Journal of Materials and Design, Vol. 288, 2007, pp. 1379-1385.
- [27] Hosseinzade, M., Mostajeran, H., Bakhshi-Jooybari, M., Gorji, AH., Norouzi, S., and Hosseinipour, S. J. “Novel combined standard hydromechanical sheet hydroforming process”, Proc IMechE B Journal of Engineering Manufacture, Vol. 224, 2010, pp. 447-457..